Available online at www.sciencedirect.com
ScienceDirect
International Journal of Solids and Structures 45 (2008) 2976–2992
INTERNATIONAL JOURNAL OF SOLIDS AND STRUCTURES
www.elsevier.com/locate/ijsolstr

The use of conservative integral in bi-material interface crack problems subjected to thermal loads

Ratnesh Khandelwal, J.M. Chandra Kishen *

Department of Civil Engineering, Indian Institute of Science, Bangalore 560 012, India

Received 3 September 2007; received in revised form 11 December 2007
Available online 15 January 2008

Abstract

A linear bi-material elastic body containing a crack at the interface and subjected to thermal loading is analyzed. The J_2 line integral, developed for mechanical loads by Khandelwal and Chandra Kishen [Khandelwal, Chandra Kishen, J.M., 2006. Complex variable method of computing J_k for bi-material interface cracks. Engineering Fracture Mechanics 73, 1568–1580] is extended to thermal loading. This method, used in conjunction with the finite element method, is shown to be useful in the prediction of stress intensity factors for cracks lying at the interface of two dissimilar materials and subjected to any type of thermal loading.

Keywords: Bi-material interface; Conservation integral; Stress intensity factors; Thermal load

1. Introduction

The study of thermal stress fracture problems arising out of the local intensification of temperature gradient is of considerable practical importance, especially, in the design of turbines, combustion chambers, nuclear reactors, etc. Further, in technologically challenging applications such as nuclear pressure vessel and piping, the existing cracks may be subjected to severe thermal environments. When the heat flow is disturbed by presence of the cracks, there is local intensification of thermal gradients accompanied by intensified thermal stresses (Sih, 1962) which may lead to the crack propagation or eventual breakdown of the structure. Hence, to insure the safety of structures under thermal loadings, an accurate thermal fracture mechanics analysis is required. This requires the determination of stress intensity factors (SIFs) due to thermal loads.

To determine the stress intensity factors due to thermal effect in a homogenous elastic body, Wilson and Yu (1979) proposed a modification to the conventional J integral. The J integral was extended to 3D thermal problems by Shih et al. (1986). Stern (1979) used the concept of reciprocal work integral to develop an analytical solution for bi-material thermal fracture problems. Lee and Shul (1991) presented an analytical solution

* Corresponding author. Tel.: +91 80 22933117; fax: +91 80 23600404.
E-mail address: chandrak@civil.iisc.ernet.in (J.M. Chandra Kishen).

0020-7683/$ - see front matter © 2008 Elsevier Ltd. All rights reserved.
doi:10.1016/j.ijsolstr.2008.01.006

for bi-material body subjected to far field heat flux. Wilson and Meguid (1995) employed thermal J-integrals along with the mode separation concept given by Ishikawa et al. (1979) in order to calculate thermal stress intensity factors. Yuuki and Cho (1989) have applied the stress extrapolation method (SE) and the displacement extrapolation method(DE) to an interface crack between dissimilar materials. Sun and Quin (1997) have recommended the use of modified crack closure integral along with displacement ratio method (DR) for better accuracy in the computation of stress intensity factors. Sun and Ikeda (2001) have modified the Virtual crack extension method and the modified crack closure integral method for thermal problem in conjunction with the superposition method to obtain thermal stress intensity factors.

There are different ways to calculate complex stress intensity factors. One is based on the concept of J_k line integral theory presented by Khandelwal and Chandra Kishen (2006). Alternative methods such as domain integrals and interaction integrals are also well suited for SIF calculation. Building upon the domain integral method, Moran and Shih (1987) and Shih and Asaro (1988) employed a domain representation of an interaction integral to directly extract complex stress intensity factors for interface cracks in linear elastic solid. Shih et al. (1988), Nakamura (1991), Lo et al. (1994), and Nakamura and Kushner (1995) have extended the above interaction integrals to 3D interface cracks, dynamically propagating cracks and cracks in composite laminates. Very recently Banks-Sills and Dolev (2004) extended conservative M_1 integral or the interaction integral into domain integral form to treat the thermo-elastic bi-material problems. The domain form of the interaction integral circumvent the need to capture the details of the singular fields near the crack tip, enabling the user to obtain accurate solutions even when coarse meshes are used.

However, for implementation of the domain integral method in existing finite element programs through post-processing operations, significant amount of effort is required. Although few commercial softwares, such as ABAQUS, Version 6.7 and WARP3D-Release 15 (2004) have built-in subroutines to compute the domain integrals, many of the finite element analysis (FEA) software do not have this capability. On the other hand, J_2, on account of existence of J_1 integral in these FEA softwares, is much easier to implement in comparison to the domain integral approach.

In the J_k integral method, part of the computation deals with the local singular stress field near the crack tip, and hence the accuracy of J_2 and the corresponding SIF computation is a concern. This work modifies the concept of J_k integral for thermal loads and investigates the computational error by comparing the results with the exact solutions available in literature.

The subject of path-independent integrals (J_k) of fracture mechanics has received considerable attention from researchers (Eischen, 1987; Chang and Pu, 1997) with regard to numerical determination of the Mixed-Mode stress intensity factors. Khandelwal and Chandra Kishen (2006) have proposed the analytical expression for J_k integral for bi-material interface problems subjected to mechanical loading. It has been shown in Khandelwal and Chandra Kishen (2006) that this integral is path independent in a modified sense and is useful in the determination of stress intensity factors. J_k integrals are line integrals evaluated along a counterclockwise contour enclosing and shrinking onto the crack tip. Knowles and Sternberg (1972) have defined J_k, $k = 1, 2$ as a complex quantity given by

$$J = J_1 - \mathrm{i}J_2 \tag{1}$$

The quantity J corresponds to the energy release rate for movement of crack edge in any direction. For homogeneous media with traction free crack surface, J_1 can start anywhere from the lower crack surface and end anywhere along the upper crack surface. The same does not hold true for J_2, wherein two additional line integrals along the crack surfaces are added up and causes the inclusion of a singular region in the integration. Therefore, direct calculation of J_2 from numerical solution is not possible in a straight forward manner. Nevertheless, J_2 was proven to be of great importance in fracture analysis, especially in predicting the kinking direction for crack extension (Hellen and Blackburn, 1975). To overcome the difficulty in computing J_2, an approximate expression have been proposed for isotropic (Eischen, 1987) and anisotropic (Chang and Pu, 1997) elastic materials. The present study shows that, in the presence of thermal stresses, the J_k line integral over a closed path, which does not enclose singularities, is not equal to zero. Instead, it is equal to an integral taken over the area inside the closed path. A method is proposed to compute the stress intensity factors for bi-material interface crack subjected to thermal loading by combining this area integral with the J_k integral. The proposed method is validated for benchmark problems available in the literature.

2. Formulation

J integral for the thermal case was first given by Wilson and Yu (1979) wherein it has been assumed that the body is subjected to thermal load without giving any consideration to body forces. It may be noted that in the derivation of any analytical form for thermo-elastic problems from mechanical load case, the presence of body forces also need to be considered. This is because, both, the body forces without any thermal loads and with thermal loads, are related to each other through the body analogy concept (Boley and Weiner, 1962). In this section, the presence of body forces is incorporated in the derivation of J_k integral subjected to thermal load. The path-independent integral J_k, $k = 1, 2$ for an elastic isothermal homogeneous material in the absence of body forces and thermal loading can be expressed as

$$J_k = \lim_{\rho \to 0} \oint_{\Gamma_\rho} (W^{\mathrm{el}} n_k - \sigma_{ij} u_{i,k} n_j) \mathrm{d}\Gamma \tag{2}$$

where W^{el} is the elastic strain energy density and in the present isothermal case is equal to the total strain energy density, W^{T}, since both, the elastic and total strains are equal in isothermal cases. n_k is the unit outward normal of Γ_ρ (Fig. 1), u_i is the displacement in the cartesian coordinate system, σ_{ij} is the stress tensor and $\mathrm{d}\Gamma$ is the arc length measured along the contour Γ_ρ.

Here,

$$W^{\mathrm{el}} = \int_0^{\epsilon^{\mathrm{el}}} \sigma_{ij} \, \mathrm{d}\epsilon_{ij}^{\mathrm{el}} \tag{3}$$

$$W^{\mathrm{T}} = W^{\mathrm{el}} = \frac{1}{2} \sigma_{ij} \epsilon_{ij} \tag{4}$$

where ϵ_{ij} is the total strain and in the present case is equal to elastic strain $\epsilon_{ij}^{\mathrm{el}}$. σ_{ij} may be represented as

$$\sigma_{ij} = \lambda \epsilon_{kk} \delta_{ij} + 2\mu \epsilon_{ij} \tag{5}$$

where δ_{ij} is the Kronecker delta function defined as follows

$$\delta_{ij} = \begin{cases} 1 & \text{when } i = j \\ 0 & \text{when } i \neq j \end{cases} \tag{6}$$

μ is shear modulus and λ is Lame's constant which is given by

$$\begin{aligned} &\lambda = \tfrac{vE}{(1+v)(1-2v)} && \text{for plane strain} \\ &\lambda = \tfrac{vE}{(1-v^2)} && \text{for plane stress} \end{aligned} \tag{7}$$

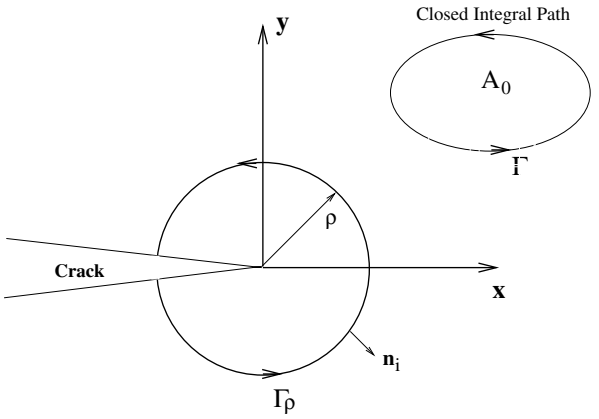

Fig. 1. Integration path Γ_ρ for conservative integral J_k in a homogenous body.

Here E is the modulus of elasticity and ν the Poisson's ratio. In the presence of thermal loads, the stress field is modified and can be written in the Duhamel Neumann contitutive equation as

$$\sigma_{ij} = \lambda\epsilon_{kk}\delta_{ij} + 2\mu\epsilon_{ij} - \beta\theta\delta_{ij} \quad i,j = 1,2 \tag{8}$$

If α be the coefficient of thermal expansion then β is defined as

$$\begin{aligned} &\beta = \tfrac{E\alpha}{(1-2\nu)} \quad \text{for plane strain} \\ &\beta = \tfrac{E\alpha}{(1-\nu)} \quad \text{for plane stress} \end{aligned} \tag{9}$$

It may be mentioned here that, in the presence of body forces and thermal loads, the total strain energy density W^{T} is still related to the stress and strain tensors as given by Eq. (4). However, in this case, the elastic strain energy density W^{el} of the system is different from total strain energy density W^{T}. W^{el} and W^{T} are related by

$$W^{\mathrm{el}} = \frac{1}{2}\sigma_{ij}(\epsilon_{ij} - \alpha\theta\delta_{ij}) = W^{\mathrm{T}} - \frac{1}{2}\alpha\theta\sigma_{ii} \tag{10}$$

Substituting for σ_{ii} from Eq. (8), we obtain

$$\begin{aligned} &W^{\mathrm{el}} = W^{\mathrm{T}} - \tfrac{\beta\theta}{2}\epsilon_{kk} + \beta\alpha\theta^2 \quad \text{for plane stress} \\ &W^{\mathrm{el}} = W^{\mathrm{T}} - \tfrac{\beta\theta}{2(1+\nu)}\epsilon_{kk} + \beta\alpha\theta^2 \quad \text{for plane strain} \end{aligned} \tag{11}$$

The line integral of Eq. (2) which is conservative in form, when applied to an arbitrary closed integral path Γ, enclosing a portion of the solid free of any material and geometric discontinuity, can be converted into an area integral using the Divergence theorem and is given by

$$J_k = \int_{A_0}\left[\frac{\partial W^{\mathrm{el}}}{\partial x_k} - \frac{\partial}{\partial x_j}\left(\sigma_{ij}\frac{\partial u_i}{\partial x_k}\right)\right]\mathrm{d}A \tag{12}$$

where A_0 is the area enclosed by the closed path Γ. Here, if the body is free from any thermal and body forces then Eq. (12) reduces to zero (Knowles and Sternberg, 1972).

In the presence of body forces and mechanical loads, the strain energy can be represented solely as a function of the strain components. Using the chain rule of differentiation it can be written as,

$$\frac{\partial W^{\mathrm{el}}}{\partial x_k} = \frac{\partial W^{\mathrm{el}}}{\partial \epsilon_{ij}}\frac{\partial \epsilon_{ij}}{\partial x_k} = \sigma_{ij}\frac{\partial}{\partial x_k}\left(\frac{\partial u_i}{\partial x_j}\right) \tag{13}$$

Using the equilibrium equations in the presence of body force f_i and switching indices, Eq. (13) can be re-written as

$$\frac{\partial W^{\mathrm{el}}}{\partial x_k} = \frac{\partial}{\partial x_j}\left(\sigma_{ij}\frac{\partial u_i}{\partial x_k}\right) + f_i\frac{\partial u_i}{\partial x_k} \tag{14}$$

From Eqs. (12) and (14), we obtain

$$J_k = \int_{A_0} f_i\frac{\partial u_i}{\partial x_k}\,\mathrm{d}A \tag{15}$$

Eq. (15) is the resulting equation for J_k in the presence of body forces. This implies that for the J_k integral defined by Eq. (2) to be zero around any closed path in the presence of body forces, the above area integral should be subtracted from it. Thus, the modified J_k integral around a closed path in the presence of body forces would be

$$\oint_{\Gamma}(W^{\mathrm{el}}n_k - \sigma_{ij}u_{i,k}n_j)\mathrm{d}\Gamma - \int_{A_0} f_i\frac{\partial u_i}{\partial x_k}\,\mathrm{d}A = 0 \tag{16}$$

However, the objective of the present study is to obtain the expression for J_k when thermal loading is present. To obtain the thermal-elastic expression, the body force analogy (Boley and Weiner, 1962) has been used. According to this analogy, the total strains and displacements of a body subjected to thermo-elastic forces are identical to those of the same body without thermal loads but subjected to the corresponding body forces and

tractions. As shown in Fig. 2, let θ be the change in temperature, f_i, T_i and σ_{ij} are the body force components, applied tractions and stress tensor in the presence of thermal loads while $\tilde{f}_i$, $\tilde{T}_i$ and $\tilde{\sigma}_{ij}$ are the corresponding quantities in the absence of thermal loads. The analogous relationship between the two field parameters are given by

$$\begin{aligned}\tilde{f}_i &= f_i - \beta\theta_{,i}\\ \tilde{\sigma}_{ij} &= \sigma_{ij} + \beta\theta\delta_{ij}\\ \tilde{T}_i &= T_i + \beta\theta n_i\end{aligned} \tag{17}$$

where, β is as defined in Eq. (9), n_i is the component of the unit normal in the x_i direction.

In an isothermal case, the total strain ($\tilde{\epsilon}_{ij}$) is equal to the elastic strain ($\tilde{\epsilon}^{el}_{ij}$) and since the body analogy method keeps the total strain in the isothermal ($\tilde{\epsilon}_{ij}$) and non-isothermal (ϵ_{ij}) cases equal, Eq. (16) can be re-written as,

$$\oint_\Gamma \left(\frac{1}{2}\tilde{\sigma}_{ij}\epsilon_{ij}n_k - \tilde{T}_i u_{i,k}\right)\mathrm{d}\Gamma - \int_{A_0}\tilde{f}_i\frac{\partial u_i}{\partial x_k}\,\mathrm{d}A = 0 \tag{18}$$

Replacing the field parameters in the above equation with a corresponding analogous body subjected to thermal loads by making use of Eq. (17), we obtain

$$\oint_\Gamma \left(\frac{1}{2}\sigma_{ij}\epsilon_{ij}n_k - T_i u_{i,k}\right)\mathrm{d}\Gamma + \oint_\Gamma \left(\frac{1}{2}\beta\theta\epsilon_{ii}n_k - \beta\theta n_i u_{i,k}\right)\mathrm{d}\Gamma - \int_{A_0} f_i\frac{\partial u_i}{\partial x_k}\,\mathrm{d}A + \int_{A_0}\beta\frac{\partial\theta}{\partial x_i}\frac{\partial u_i}{\partial x_k}\,\mathrm{d}A = 0 \tag{19}$$

Making use of the divergence theorem, the second integral of Eq. (19) can be reduced and written as

$$\oint_\Gamma \left(\frac{1}{2}\beta\theta\epsilon_{ii}n_k - \beta\theta n_i u_{i,k}\right)\mathrm{d}\Gamma = \int_{A_0}\left(-\frac{\beta}{2}(\theta\epsilon_{ii})_{,k} + \beta\epsilon_{ii}\theta_{,k} - \beta u_{i,k}\theta_{,i}\right)\mathrm{d}A \tag{20}$$

$$\oint_\Gamma (W^{\mathrm{T}}n_k - \sigma_{ij}u_{j,k}n_i)\mathrm{d}\Gamma - \int_{A_0}(f_i u_{i,k})\mathrm{d}A - \beta\int_{A_0}\left(\frac{1}{2}(\theta\epsilon_{ii})_{,k} - \epsilon_{ii}\theta_{,k}\right)\mathrm{d}A = 0 \tag{21}$$

In the absence of body forces Eq. (21) can be written as,

$$\oint_\Gamma (W^{\mathrm{T}}n_k - \sigma_{ij}u_{j,k}n_i)\mathrm{d}\Gamma - \beta\int_{A_0}\left(\frac{1}{2}(\theta\epsilon_{ii})_{,k} - \epsilon_{ii}\theta_{,k}\right)\mathrm{d}A = 0 \tag{22}$$

Considering two elastic half planes of different materials bounded together as shown in Fig. 3, Γ^1 and Γ^2 are closed contours taken arbitrarily in the anticlockwise direction with the contact points on crack surface and interface at the same distance from the crack tip. The inner paths, $\Gamma_{\rho 1}$ and $\Gamma_{\rho 2}$ are semi-circular anticlockwise contours having the same radius ρ about the crack tip. Now, Γ can be written as $\Gamma = \Gamma^1 + \Gamma^2$, where $n = 1, 2$ and $\Gamma^2 = \Gamma_c^- + \Gamma_2 + \Gamma_l^- - \Gamma_{\rho 2}$ and $\Gamma^1 = \Gamma_l^+ + \Gamma_1 + \Gamma_c^+ - \Gamma_{\rho 1}$.

The plane defined by $x < 0$ and $y = 0$ is unbounded and represents a crack. The material occupying $y > 0$ has Young's modulus E_1, Poisson's ratio v_1 and thermal expansion coefficient α_1 whereas that occupying $y < 0$

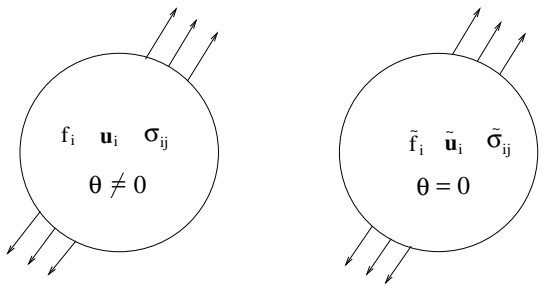

Fig. 2. Analogous bodies with and without thermal loads.

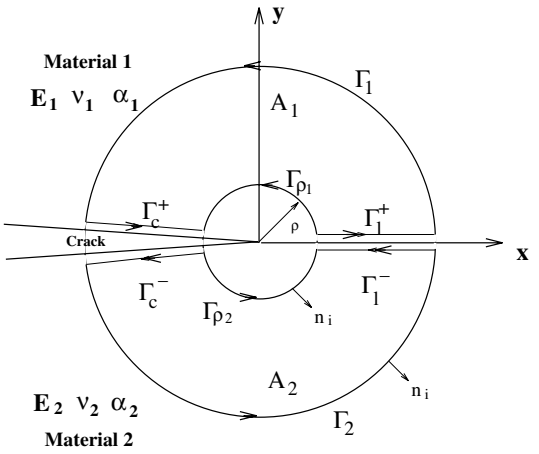

Fig. 3. Integration path Γ for conservative integral J_k in a bi-material body.

has the respective values as E_2, ν_2 and α_2. Application of the conservation law given in Eq. (22) to the upper and lower closed loops Γ^1 and Γ^2 (Fig. 3), separately results in

$$\begin{aligned}
&\oint_{\Gamma_l^+ + \Gamma_1 + \Gamma_c^+ - \Gamma_{\rho 1}} (W^{\mathrm{T}} n_k - \sigma_{ij} u_{j,k} n_i) \mathrm{d}\Gamma - \beta_1 \int_{A_1} \left(\frac{1}{2} (\theta \epsilon_{ii})_{,k} - \epsilon_{ii} \theta_{,k} \right) \mathrm{d}A = 0 \\
&\oint_{\Gamma_c^- + \Gamma_2 + \Gamma_l^- - \Gamma_{\rho 2}} (W^{\mathrm{T}} n_k - \sigma_{ij} u_{j,k} n_i) \mathrm{d}\Gamma - \beta_2 \int_{A_2} \left(\frac{1}{2} (\theta \epsilon_{ii})_{,k} - \epsilon_{ii} \theta_{,k} \right) \mathrm{d}A = 0
\end{aligned} \tag{23}$$

where A_1 and A_2 represent the area enclosed within the upper and lower closed loops Γ^1 and Γ^2, respectively. For the sake of simplicity in writing of equations, let us define,

$$L = W^{\mathrm{T}} n_k - \sigma_{ij} u_{j,k} n_i$$

Combining the integrals along Γ_1 and Γ_2 into one term Γ_0 and also the integrals along $\Gamma_{\rho 1}$ and $\Gamma_{\rho 2}$ into Γ_ρ and rewriting Eqs. (23)

$$\begin{aligned}
\oint_{\Gamma_\rho} (W^{\mathrm{T}} n_k - \sigma_{ij} u_{j,k} n_i) \mathrm{d}\Gamma = &\int_{\Gamma_c^+ + \Gamma_c^-} (L) \mathrm{d}\Gamma + \int_{\Gamma_l^+ + \Gamma_l^-} (L) \mathrm{d}\Gamma + \oint_{\Gamma_0} (L) \mathrm{d}\Gamma \\
&- \sum_{m=1}^{2} \beta_m \int_{A_m} \left[\frac{1}{2} (\theta \epsilon_{ii})_{,k} - \epsilon_{ii} \theta_{,k} \right] \mathrm{d}A
\end{aligned} \tag{24}$$

J_k integral is defined with its first part in terms of elastic strain energy density W^{el}. Converting W^{T} of left hand side of the Eq. (24) to W^{el} using Eq. (10) and taking limit $\rho \to 0$

$$\begin{aligned}
\lim_{\rho \to 0} \oint_{\Gamma_\rho} (W^{\mathrm{el}} n_k - \sigma_{ij} u_{j,k} n_i) \mathrm{d}\Gamma = &\int_{\Gamma_c^+ + \Gamma_c^-} (L) \mathrm{d}\Gamma + \int_{\Gamma_l^+ + \Gamma_l^-} (L) \mathrm{d}\Gamma + \oint_{\Gamma_0} (L) \mathrm{d}\Gamma - \lim_{\rho \to 0} \sum_{m=1}^{2} \frac{1}{2} \alpha_m \oint_{\Gamma_{\rho m}} \theta \sigma_{ii} n_k \mathrm{d}\Gamma \\
&- \sum_{m=1}^{2} \beta_m \int_{A_m} \left[\frac{1}{2} (\theta \epsilon_{ii})_{,k} - \epsilon_{ii} \theta_{,k} \right] \mathrm{d}A
\end{aligned} \tag{25}$$

The first term of the area integrand of Eq. (25) can be transformed back to line integral using Green's theorem and can be clubbed together along with integrands of different integrals along the parts of the complete path Γ. Rewriting Eq. (25) by making use of Eq. (2)

$$J_k = \int_{\Gamma_c^+ + \Gamma_c^-} (L_1)\mathrm{d}\Gamma + \int_{\Gamma_l^+ + \Gamma_l^-} (L_1)\mathrm{d}\Gamma + \oint_{\Gamma_0} (L_1)\mathrm{d}\Gamma + \sum_{m=1}^{2} \beta_m \int_{A_m} \epsilon_{ii}\theta_{,k}\,\mathrm{d}A - \lim_{\rho\to 0} \sum_{m=1}^{2} \oint_{\Gamma_{\rho_m}} \left[\frac{\alpha_m}{2}\theta\sigma_{ii} - \frac{\beta_m}{2}\theta\epsilon_{ii}\right] n_k\,\mathrm{d}\Gamma \tag{26}$$

where L_1 is defined as

$$L_1 = \left(W^{\mathrm{T}} - \frac{\beta}{2}\theta\epsilon_{ii}\right) n_k - \sigma_{ij}u_{j,k}n_i = W_F n_k - \sigma_{ij}u_{j,k}n_i$$

The last integral on the right hand side of the Eq. (26) tends to zero as $\rho \to 0$ and hence can be neglected. Also, the conditions along straight crack surface and interface which are parallel to x-axis requires the following conditions to be satisfied:

1. $n_1 ds = dy = 0$
2. $n_2 = +1$ for Γ_c^- and Γ_l^-
3. $n_2 = -1$ for Γ_c^+ and Γ_l^+
4. For traction free crack surfaces $\sigma_{ij}n_i = 0$
5. Continuity conditions of displacements and tractions across the interface requires $[\![\, u_j \,]\!] = 0$ and $[\![\, \sigma_{j2} \,]\!] = 0$

For the limit case consisting in $\Gamma_{\rho\to 0}$ the left hand side of Eq. (26) can be reduced to the well known J integral (J_1 in present case) for $k = 1$. Further for $k = 2$, Eq. (26) does not converge to some fixed value and is defined for some very small value of ρ lying within the singularity dominated zone and is defined here as the $J_{2\rho}$ integral whose analytical expression has been given in Khandelwal and Chandra Kishen (2006).

$$J_1 = \oint_{\Gamma_0} (W_F n_1 - \sigma_{ij}u_{j,1}n_i)\mathrm{d}\Gamma + \sum_{k=1}^{2} \beta_k \int_{A_k} \theta_{,1}\epsilon_{ii}\,\mathrm{d}A \tag{27}$$

$$J_{2\rho} = \oint_{\Gamma_0} (W_F n_2 - \sigma_{ij}u_{j,2}n_i)\mathrm{d}\Gamma + \int_{\Gamma_c^+ + \Gamma_c^-} W_F n_2 \mathrm{d}\Gamma + \int_{\Gamma_l^+ + \Gamma_l^-} (W_F - \sigma_{j2}u_{j,2})n_2\,\mathrm{d}\Gamma + \sum_{k=1}^{2} \beta_k \int_{A_k} \theta_{,2}\epsilon_{ii}\,\mathrm{d}A \tag{28}$$

The expressions for J_1 and J_2 integrals or the limiting case of the left hand side of Eqs. (27) and (28) for the limit as $\Gamma_{\rho\to 0}$ can be written as (Khandelwal and Chandra Kishen, 2006)

$$J_1 = \left[\frac{(1+\kappa_1)}{16\mu_1} + \frac{(1+\kappa_2)}{16\mu_2}\right](K_1^2 + K_2^2) \tag{29}$$

$$J_{2\rho} = -\frac{1}{32\pi\varepsilon}\left[\frac{(1+\kappa_1)}{\mu_1}(1 - \mathrm{e}^{-2\pi\varepsilon}) + \frac{(1+\kappa_2)}{\mu_2}(\mathrm{e}^{2\pi\varepsilon} - 1)\right]\left[(K_1^2 - K_2^2)\sin 2\varepsilon\log(\rho) + 2K_1K_1\cos(2\varepsilon\log\rho)\right] \tag{30}$$

where μ_j is the shear modulus of material j, $\kappa_j = (3 - \nu_j)/(1 + \nu_j)$ for plane stress and $\kappa_j = 3 - 4\nu_j$ for plane strain. ν_j is Poisson's ratio of material j and ε is the bi-materials constant defined by

$$\varepsilon = \frac{1}{2\pi}\ln\left[\frac{\kappa_1\mu_2 + \mu_1}{\kappa_2\mu_1 + \mu_2}\right] \tag{31}$$

2.1. Computation of bi-material stress intensity factors

The main objective of this work is to compute the stress intensity factors for bi-material interface cracks when subjected to thermal loads and this is done using the above definitions of J_1 and $J_{2\rho}$.

Eqs. (29) and (30) can be written in the form

$$(K_1^2 + K_2^2) = B_1 J_1 \tag{32}$$

$$(K_1^2 - K_2^2)C_1 + 2K_1K_2C_2 = J_{2\rho} \tag{33}$$

where

$$\frac{1}{B_1} = \left[\frac{(1+\kappa_1)}{16\mu_1} + \frac{(1+\kappa_2)}{16\mu_2}\right]$$

$$C_1 = -\frac{1}{32\pi\epsilon}\left[\frac{(1+\kappa_1)}{\mu_1}(1-e^{-2\pi\epsilon}) + \frac{(1+\kappa_2)}{\mu_2}(e^{2\pi\epsilon}-1)\right]\sin(2\epsilon\log\rho)$$

$$C_2 = -\frac{1}{32\pi\epsilon}\left[\frac{(1+\kappa_1)}{\mu_1}(1-e^{-2\pi\epsilon}) + \frac{(1+\kappa_2)}{\mu_2}(e^{2\pi\epsilon}-1)\right]\cos(2\epsilon\log\rho)$$

Elimination of K_2 from Eqs. (32) and (33) results in

$$K_1^4(4C_1^2 + 4C_2^2) - 4K_1^2\left[J_1B_1(C_1^2 + C_2^2) + J_{2\rho}C_1\right] + (J_1B_1C_1 + J_{2\rho})^2 = 0 \tag{34}$$

Hence, K_1 can be obtained by solving the above equation. Substituting for K_1 in Eq. (32), we can compute K_2.

The sign of K_1 and K_2 are determined by monitoring the magnitude of the crack opening displacement near the crack tip. The crack opening displacement may be defined as

$$\Delta u = u^+ - u^- \tag{35}$$

$$\Delta v = v^+ - v^- \tag{36}$$

where the + and − sign refers to the upper and lower crack faces, respectively. The signs of K_1 and K_2 correspond to the signs of Δu and Δv.

3. Validation

In order to validate the above formulation, three benchmark problems of plane stress, one under uniform temperature and other two under thermal flow are considered. Finite element analysis are performed using the program ANSYS (2005) with eight-noded isoparametric elements, PLANE82 for elastic analysis and PLANE77 for thermal analysis. The line integral calculation of both, J_1 and $J_{2\rho}$ have been computed using a newly developed post-processing macro in the finite element program. The area integral part of J_1 and $J_{2\rho}$ have been computed using the Gauss point average values by summing up the Gauss point quantities for each element, averaged and multiplied by the elemental area.

A convergence study is performed for the problems considered in order to determine the sensitivity of mesh refinement on the results. Based on this study, an optimized mesh size is used for computation of the J_k integrals. Mesh refinement is done in the region surrounding the crack tip for the body subjected to thermal loads. In the region away from the crack tip an uniform mesh is used.

3.1. Dissimilar semi-infinite plate with double edge crack subjected to uniform temperature change

A jointed dissimilar semi-infinite plate with double edge crack subjected to uniform temperature change of 100 °C (Sun and Ikeda, 2001) is analyzed under plane stress conditions. The geometry of the plate is as shown in Fig. 4. Due to symmetry in geometry and loading about the Y-axis, only the left half is analyzed. The dimensions of the plate are taken as 200 units by 400 units with the jointed interface of 1 unit length. The material properties used in the analysis are shown in Table 1 and are assumed to be independent of temperature variation.

Results of the convergence study on this problem is shown in Fig. 5. For a value of $\rho = 7.46e{-}3$, it is shown that with increasing mesh density, calculated $J_{2\rho}$ using FE, converges to analytically obtained value. It has been observed that for mesh using 18,000 to 25,000 number of elements, there is little variation in calculated $J_{2\rho}$. The variation in computed J_1 is found to within 1% of the analytical value for all the mesh sizes considered in this study. As a tradeoff between solution accuracy and computation time, a FE mesh of 20,494 eight-noded elements with 62,245 nodes have been used for subsequent analysis. Figs. 6 and 7 show the finite ele-

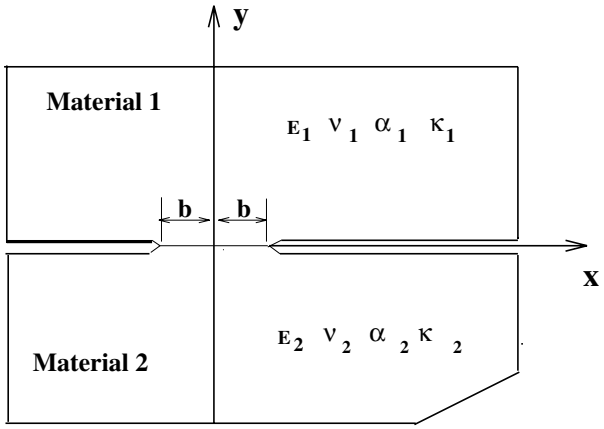

Fig. 4. Jointed dissimilar semi-infinite plate under constant uniform temperature of 100 °C.

Table 1
Material properties used in the analysis

Properties	Material-1	Material-2
Young modulus (Pa)	1000e9	100e9
Poisson ratio	0.3	0.3
Temperature (°C)	100	100
Coefficient of thermal expansion (/°C)	1.0e−06	1.0e−07
Coefficient of heat conduction (W/m °C)	100	100

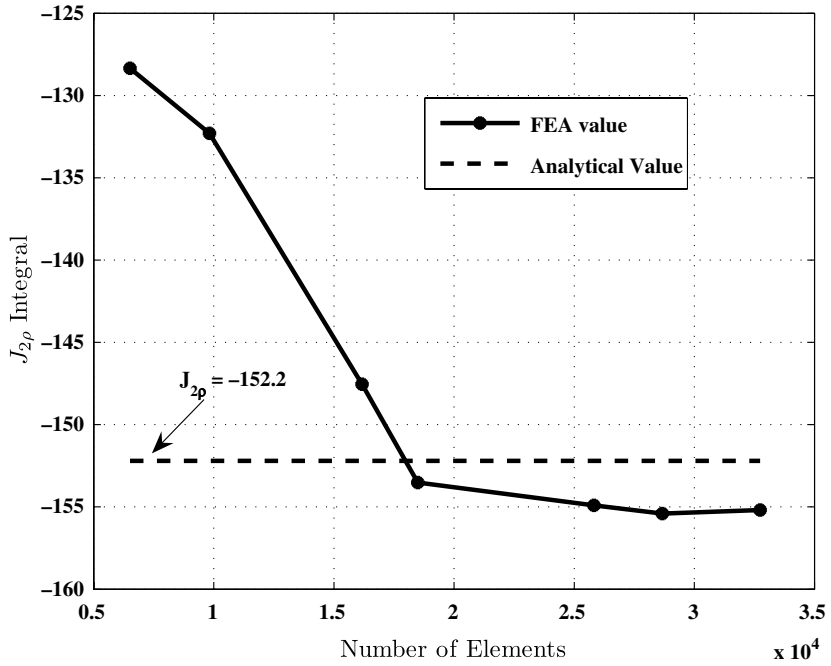

Fig. 5. Influence of mesh refinement on $J_{2\rho}$ for jointed dissimilar semi-infinite plate with double edge crack ($\rho = 7.46e{-}3$).

ment mesh along with the contours used and displacement boundary condition, respectively. The same finite element mesh is used for thermal analysis too. The analytical solution in terms of the stress intensity factors for this problem was given by Erdogan (1965) as

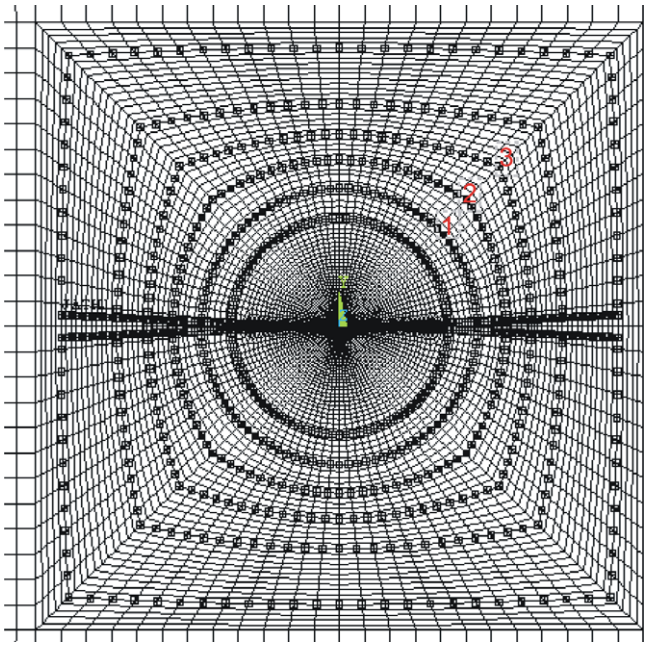

Fig. 6. A typical FE mesh and shape of the contour path used for all the problems.

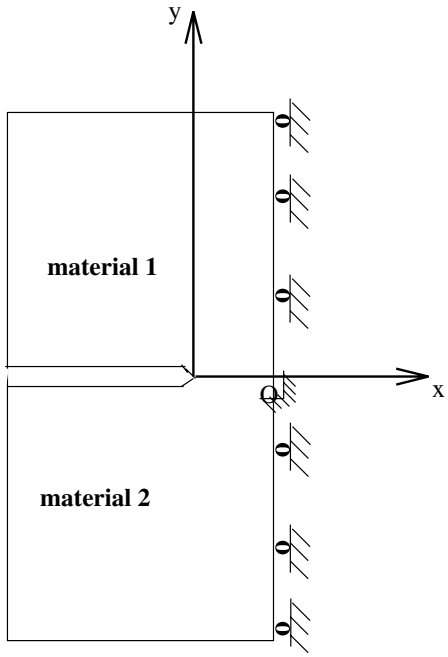

Fig. 7. Displacement boundary condition for jointed dissimilar semi-infinite plate with double edge crack under uniform temperature load.

$$K_1 = -2\epsilon\sigma_0(\alpha_2\eta_2 - \alpha_1\eta_1)\Delta T\sqrt{\pi b}(2b)^{-i\epsilon}$$
$$K_2 = \sigma_0(\alpha_2\eta_2 - \alpha_1\eta_1)\Delta T\sqrt{\pi b}(2b)^{-i\epsilon} \quad (37)$$

where, $\eta_i = 1$ for plane stress and $\eta_i = 1 + v_i$ for plane strain case, σ_0 is defined as

$$\sigma_0 = \frac{4\mu_1\mu_2\cosh(\varepsilon\pi)}{(\mu_1 + \mu_2\kappa_1 + \mu_1\kappa_2 + \mu_2)} \tag{38}$$

where α_1 and α_2 are the coefficients of linear thermal expansion for material 1 and 2, respectively. ΔT is the temperature excursion.

Let $K_0 = \sigma\sqrt{\pi b}$, where $\sigma = \sigma_0(\alpha_2\eta_2 - \alpha_1\eta_1)\Delta T$. The normalized complex stress intensity factors is defined as

$$\widetilde{K} = \frac{KL^{i\epsilon}}{\sigma\sqrt{\pi a}} \tag{39}$$

where L and a are length parameters and σ is stress. For the present case, normalized stress intensity factors with $L = 2a$ and $a = b$ can be written as

$$\widetilde{K}_1 = -2\varepsilon$$
$$\widetilde{K}_2 = 1 \tag{40}$$

Since the body is subjected to uniform temperature distribution, the area integral part in Eq. (27) becomes zero and the right hand side of this equation reduces to the line integral. Similarly, in Eq. (28), the area integral vanishes.

The J_1 and $J_{2\rho}$ integrals have been computed using a newly developed post-processing macro in the finite element program ANSYS (2005). The J_1 integral is obtained using the outer contour (Γ_1 and Γ_2 in Fig. 3) only, whereas $J_{2\rho}$ integral is computed along the outer contour (Γ_1 and Γ_2) along with material interface and crack surface (Γ_l^+, Γ_l^-, Γ_c^+ and Γ_c^- in Fig. 3). Three different contour paths are considered to demonstrate the path-independent nature of the J_1 integral. The results of the J_1 integral obtained for the three different paths along with the analytical results are shown in Table 2. It is seen that the error in the average of all the three paths of the J_1 integral is far less than one percent. Further, the variation in the computed J_1 values for the three different paths do not vary much, thus demonstrating the path independence.

Table 3 shows the results of $J_{2\rho}$ computed for four different values of the radius of inner circle, ρ, and also for three different integration paths. It is seen that the results, computed using the proposed approach, are in close agreement with the analytical results. In addition, the results do not vary much for the three different paths, again indicating the path independence even for the $J_{2\rho}$ integral.

Table 4 shows the normalized Mode I and Mode II stress intensity factors for four different values of ρ together with the analytical solutions as given by Erdogan (1965). It is seen that there is good agreement in the computed solution with an average error of 2.05% in K_1 and 0.002% in K_2.

Table 2
Results of the J_1 integral for all the three case studies

J_1	Analytical	Path_1	Path_2	Path_3	Average	% Error
Case study 1	299.3406	303.19	298.56	295.78	299.178	0.054
Case study 2	7746.746	7744.94	7740.2	7732.391	7739.18	−0.097
Case study 3	6.9698e7	6.9705e7	6.9715e7	6.9712e7	6.971e7	−0.018

Table 3
Case study 1: Results of $J_{2\rho}$ for different values of ρ

ρ	Analytical	Numerical $J_{2\rho}$			Average	% Error
	$J_{2\rho}$	Path_1	Path_2	Path_3	$J_{2\rho}$	
5.87e−3	−160.53	−165.03	−162.38	−156.52	−161.32	−0.49
7.83e−3	−150.48	−151.97	−149.2	−147.67	−149.62	0.58
9.29e−3	−144.26	−149.59	−146.7	−142.19	−146.1	−1.27
1.13e−2	−137.18	−143.2	−140.6	−132.9	−138.9	−1.25

Table 4
Case study 1: Normalized Mode I and Mode II stress intensity factors for different values of ρ

ρ	$\widetilde{K}_1$	$\widetilde{K}_2$
5.87e−3	−0.1197	1.0100
7.83e−3	−0.1242	1.0095
9.29e−3	−0.1172	1.0103
1.13e−2	−0.1176	1.0103
Average	−0.1196	1.010
Erdogan's solution	−0.12219	1.0100
% Error	2.05	−0.002

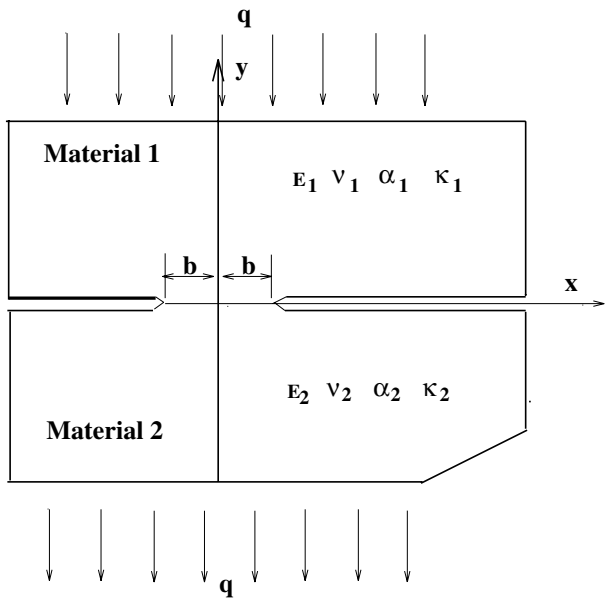

Fig. 8. Jointed dissimilar semi-infinite plate with non-insulated double edge crack under uniform thermal flow.

3.2. Jointed dissimilar semi-infinite plates with double edge cracks subjected to uniform thermal flow

In this case study, a semi-infinite bi-material plate with double edge cracks and subjected to constant heat flux of $q = 10^5$ W/m^2 in the negative Y-direction is considered (Fig. 8). The material properties are same as those considered in the previous case study as depicted in Table 1. Since the geometry of this plate and the one considered in the previous case study are the same, the same finite element mesh is used here with plane stress conditions. Fig. 9 shows left half of the geometry with displacement and thermal boundary conditions. No thermal insulation is assumed along the cracks. This is achieved by making the coincident nodes on the crack surfaces to coincide in the thermal analysis. Only during the mechanical load analysis the constraints on the nodes lying on the crack surfaces were removed.

Sun and Ikeda (2001) have solved this problem numerically using the virtual crack extension method along with the superposition principle and Banks-Sills and Dolev (2004) have solved it using the M_1 integral concept. Brown and Erdogan (1968) have presented the exact solution for the thermal stress intensity factors as

$$K_1 = \frac{\sigma_0(\alpha_2\eta_2 k_1 - \alpha_1\eta_1 k_2) qb\sqrt{\pi b}[1-4\epsilon^2]}{2k_1k_2}(2b)^{-i\epsilon}$$

$$K_2 = \frac{\sigma_0(\alpha_2\eta_2 k_1 - \alpha_1\eta_1 k_2) qb\sqrt{\pi b}(2\epsilon)}{k_1k_2}(2b)^{-i\epsilon} \tag{41}$$

where η_1, η_2 are as defined in the previous case study, k_1 and k_2 are coefficients of heat conduction, and q is the heat flow.

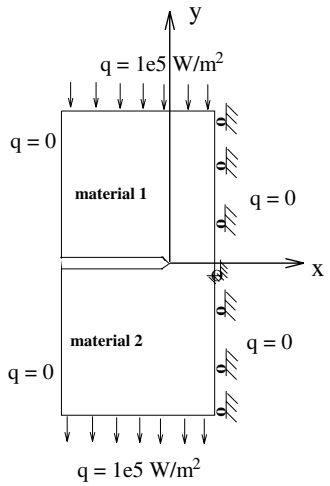

Fig. 9. Displacement and thermal boundary conditions for jointed dissimilar semi-infinite plate with non-insulated double edge crack under uniform thermal flow.

Table 5
Case study 2: Results of $J_{2\rho}$ for different values of ρ

ρ	Analytical	Numerical $J_{2\rho}$			Average	% Error
	$J_{2\rho}$	$Path_1$	$Path_2$	$Path_3$	$J_{2\rho}$	
2.68e−3	3006.105	3098.12	3071.45	2980.64	3050.07	1.46
4.17e−3	2539.04	2515.5	2495.17	2492.38	2501.02	−1.49
6.33e−3	2082.02	2048.4	2032.74	2024.34	2035.16	−2.25
9.56e−3	1618.04	1692.11	1676.23	1583.28	1650.54	2.00

Since the crack surfaces are not insulated i.e., the presence of crack does not influence the temperature distribution, the effect of far field flux on the body in negative Y direction will cause linear variation in temperature as a function of Y. Therefore, the area integral part of Eq. (27) vanishes and the whole expression on the right hand side reduces to the line integral. On the other hand, in Eq. (28) the whole area integral exist as such with temperature gradient in Y direction attaining a constant value.

The J_1 and $J_{2\rho}$ integrals have been computed as in the previous case study. Table 2 again shows the results of the J_1 integral computed for the three different paths along with analytical results.

It is seen that the error in the average of all the three paths of the J_1 integral is far less than one percent. Further, the variation in the computed J_1 values for the three different paths do not vary much, thus demonstrating the path independence.

Table 5 shows the results of $J_{2\rho}$ computed for four different values of the inner circle of radius ρ and also for three different integration paths. It is seen that the computed results are in close agreement with the analytical ones. In addition, the results do not vary much for the three different paths indicating the path independence of $J_{2\rho}$ integral.

Table 6
Case study 2: Normalized Mode I and Mode II stress intensity factors for different values of ρ

ρ	$\widetilde{K}_1$	$\widetilde{K}_2$
2.68e−3	0.4939	0.1536
4.17e−3	0.4928	0.1572
6.33e−3	0.4927	0.1576
9.56e−3	0.4937	0.1543
Average	0.4933	0.1557
Erdogan's solution	0.4885	0.1558
% Error	0.048	0.066

Table 6 shows the normalized Mode I and Mode II stress intensity factors for four different values of ρ together with the analytical values as given by Brown and Erdogan (1968). It is seen that there is good agreement in the computed solution with an average error of 0.05% in K_1 and 0.06% in K_2.

3.3. An infinite body with insulated central crack subjected to uniform thermal flow

In this case study, analysis is done on an infinite body with central insulated crack subjected to constant heat flux of $q = 10^5$ W/m^2 in the negative Y-direction under plane stress conditions as shown in Fig. 10. Both mechanical and thermal properties are considered to be the same as in the previous examples. The dimensions of semi-infinite plate is taken as 80 units by 160 units with a crack length of 4 units. Taking advantage of the symmetry in geometry and loading, only the right half of this bi-material infinite plate is modeled using ANSYS (2005).

Results of the convergence study on this problem are shown in Fig. 11. For a value of $\rho = 7.63\text{e}{-3}$, it is shown that with increasing mesh density, FE calculated $J_{2\rho}$ converges to analytically obtained value and for FE mesh using 25,000 to 30,000 number of elements there is little variation in it. As a result, FE mesh of 25,824 elements with 78,287 nodes have been used for subsequent analysis. The finite element mesh and contour path used for this problem is of the same type as shown in Fig. 6. Fig. 12 shows right half of the geometry with displacement and thermal boundary conditions. In this example, all the integrals in Eqs. (27) and (28) are non-zero and contribute to J_1 and J_2 integrals, thereby increasing the complexity of computations.

As in the previous two cases, Table 2 shows the results of J_1 integral obtained for the three different paths together with the analytical results. The analytical values shown in table for this case is obtained from computational approach of M_1 integral (Banks-Sills and Dolev, 2004).

It is seen that the error in the average of all the three paths of the J_1 integral is far less than one percent. Further, the variation in the computed J_1 values for the three different paths do not vary much, thus demonstrating the path independence.

Table 7 shows the results of $J_{2\rho}$ computed for four different values of the inner circle of radius ρ and also for three different integration paths. It is seen that the computed results are in close agreement with the analytical ones. In addition, the results do not vary much for the three different paths indicating the path independence of $J_{2\rho}$ integral.

Table 8 shows the normalized Mode I and Mode II stress intensity factors for four different values of ρ together with the analytical values obtained from the M_1 integral (Banks-Sills and Dolev, 2004). It is seen that there is good agreement in the computed solution with an average error of 0.02% in $\widetilde{K}_1$ and 1.33% in $\widetilde{K}_2$.

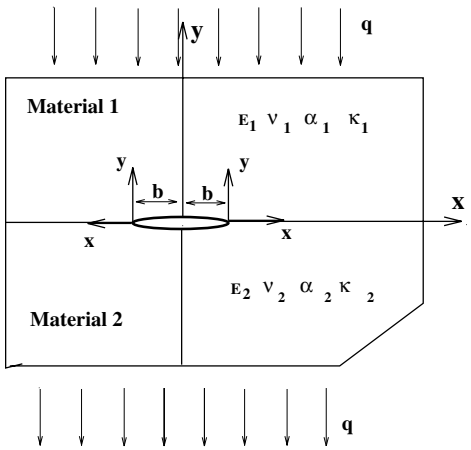

Fig. 10. Semi-infinite bi-material plate with insulated central crack under uniform thermal flow.

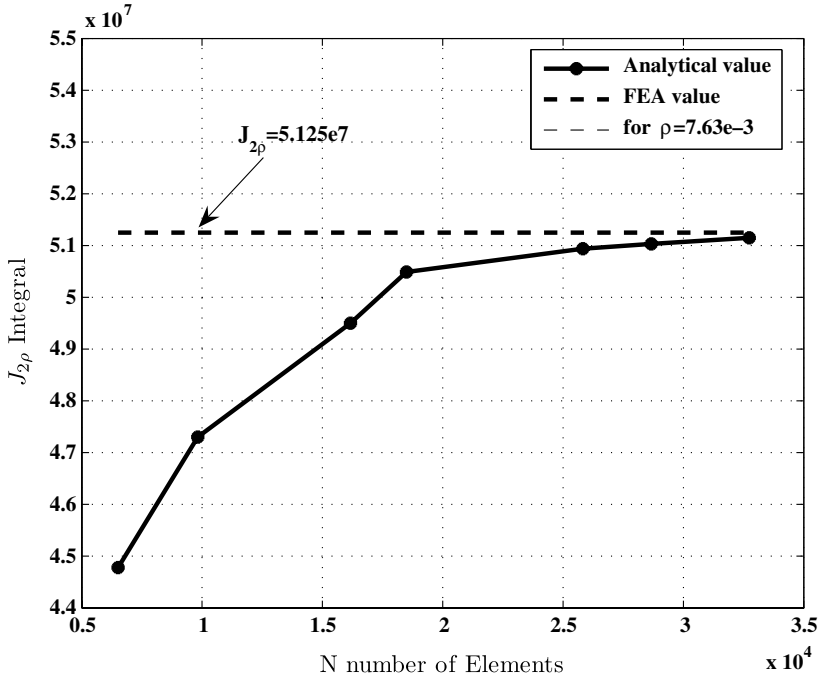

Fig. 11. Influence of mesh refinement on $J_{2\rho}$ for semi-infinite bi-material plate under uniform thermal flow ($\rho = 7.63\text{e}{-3}$).

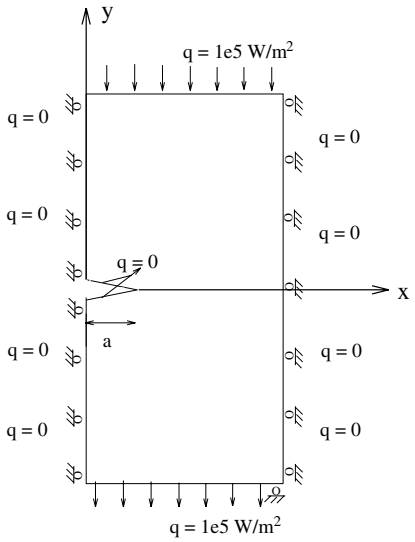

Fig. 12. Displacement and thermal boundary conditions for semi-infinite bi-material plate with insulated central crack subjected to uniform thermal flow.

Table 7
Case study 3: Results of $J_{2\rho}$ for different values of ρ

ρ	Analytical	Numerical $J_{2\rho}$			Average	% Error
	$J_{2\rho}$	Path_1	Path_2	Path_3	$J_{2\rho}$	
4.846e−3	5.309e7	5.38e7	5.36e7	5.33e7	5.358e7	0.93
7.63e−3	5.125e7	5.12e7	5.086e7	5.076e7	5.094e7	−0.603
9.68e−3	5.014e7	4.99e7	4.96e7	4.945e7	4.9635e7	−0.99
1.18e−2	4.913e7	4.915e7	4.890e7	4.892e7	4.899e7	−0.291

Table 8
Case Study 3: Normalized Mode I and Mode II stress intensity factors for different values of ρ

ρ	$\widetilde{K}_1$	$\widetilde{K}_2$
4.846e−3	−4.037	0.5017
7.63e−3	−4.0462	0.4229
9.68e−3	−4.0475	0.4107
1.18e−2	−4.0445	0.4386
Average	−4.044	0.4435
M-integral	−4.043	0.4495
% Error	−0.021	1.33

4. Conclusions

For a homogeneous crack problem, closed form expression for J_2 is available and it is physically identified as the energy release rate due to crack tip advancing normal to its original orientation. However, the same is not true for bi-material interface crack problems since it is shown to be non-existent. In the present study, it is shown that, in the presence of thermal stresses, the J_k line integral over a closed path, which does not enclose singularities, is not equal to zero, instead, it is equal to an integral taken over the area inside the closed path. A method is proposed to compute the stress intensity factors for bi-material interface crack subjected to thermal loading by combining this area integral with the J_k integral. The proposed approach has been validated using the benchmark problems with known analytical solutions and the results are found to be in very good agreement.

In order to properly characterize the near tip behavior, the cut-off radius ρ should be small enough so that the integration contour for $J_{2\rho}$ is inside the region dominated by singularity zone. It is seen that the results of K_1 and K_2 are insensitive to different selections of ρ.

References

ABAQUS unified FEA. SIMULIA, The Dassault Systems Brand for Realistic Simulation, Providence, RI, USA.

ANSYS, 2005. University Advanced, v. 10.0. ANSYS, Inc., Southpointe, 275 Technology Drive, Canonsburg, PA 15317, USA.

Banks-Sills, L., Dolev, O., 2004. The conservative *M* integral for thermal-elastic problems. International Journal of Fracture 125, 149–170.

Boley, B.A., Weiner, J.H., 1962. Theory of Thermal Stresses. Wiley, New York.

Brown, E.J., Erdogan, F., 1968. Thermal stress in bounded materials containing cuts on the interface. International Journal of Fracture 6, 517–529.

Chang, J.H., Pu, L.P., 1997. A finite element approach for J_2 calculation in anisotropic materials. Composite Structures 62 (4), 635–647.

Eischen, J.W., 1987. An improved method for calculating J_2 integral. Engineering Fracture Mechanics 26 (5), 461–472.

Erdogan, F., 1965. Stress distribution in bounded dissimilar materials with cracks. Transactions of the ASME, Journal of Applied Mechanics 32, 403–410.

Hellen, T.K., Blackburn, W.S., 1975. The stress intensity calculation for combines tensile and shear loading. International Journal of Fracture 11, 605–617.

Ishikawa, H., Kitagawa, H., Okamura, H., 1979. J integral of a mixed mode crack and its application. Mechanical Behaviour of Materials 3, 447–455.

Knowles, J.K., Sternberg, E., 1972. On a class of conservation laws in linearilized and finite elastostatics. Archive for Rational Mechanics and Analysis 44, 187–211.

Lee, K.Y., Shul, C.W., 1991. Determination of stress intensity factors for an interface crack under vertical uniform heat flow. Engineering Fracture Mechanics 40 (6), 1067–1074.

Lo, C.Y., Nakamura, T., Kushner, A., 1994. Computational analysis of dynamic crack propagation along bimaterial interface. International Journal of Solids and Structure 31, 145–168.

Moran, B., Shih, C.F., 1987. A general treatment of crack tip contour integrals. International Journal of Fracture 35, 295–310.

Nakamura, T., 1991. Three-dimensional stress fields of elastic interface cracks. Transactions of the ASME, Journal of Applied Mechanics 58 (4), 939–946.

Nakamura, T., Kushner, A.L.C.Y., 1995. Interlaminar dynamic crack propagation. International Journal of Solids and Structure 32, 2657–2675.

Khandelwal, Ratnesh, Chandra Kishen, J.M., 2006. Complex variable method of computing J_k for bi-material interface cracks. Engineering Fracture Mechanics 73, 1568–1580.

Shih, C.F., Asaro, R.J., 1988. Elastic-plastic analysis of cracks on bi-material interface: Part-*I*, small scale yielding. Transactions of the ASME, Journal of Applied Mechanics 55, 299–316.

Shih, C.F., Moran, B., Nakamura, T., 1986. Energy release rate along three dimension crack front in a thermally stress body. International Journal of Fracture 30, 79–102.

Shih, C.F., Moran, B., Nakamura, T., 1988. Crack tip integrals and domain integral representation for three-dimensional crack problems. In: Rosakis, A.J., Ravi-Chandar, K., Rajapakse, Y. (Eds.), Analytical, Numerical and Experimental Aspects of Three Dimensional Fracture Processes. American Society of Mechanical Engineering, New York, NY, p. AMD 91.

Sih, G.C., 1962. On the singular character of thermal stress near a crack tip. Transactions of the ASME, Journal of Applied Mechanics 29, 587–588.

Stern, M., 1979. The numerical calculation of thermally induced stress intensity factor. Journal of Elasticity 9, 91–95.

Sun, C.T., Ikeda, T., 2001. Stress intensity factor analysis for an interface crack between dissimilar isotropic materials under thermal stress. International Journal of Fracture 111, 229–249.

Sun, C.T., Quin, W., 1997. The use of finite extension strain energy release rates in fracture of interfacial cracks. International Journal of Solids and Structure 34, 2595–2609.

WARP3D-Release 15, 2004. 3-D Dynamic Nonlinear Fracture Analysis of Solids Using Parallel Computers and Workstations. Authors: Arne Gullerud, Kyle Koppenhoefer, Arun Roy, Sushovan RoyChowdhury, Matt Walters, Barron Bichon, Kristine Cochran, Robert H. Dodds, Jr., Department of Civil Engineering, University of Illinois at Urbana-Champaign, Urbana, IL, USA.

Wilson, R.I., Meguid, S.A., 1995. On the determination of mixed mode stress intensity factors of an angled cracks in a disc using FEM. Finite Element in Analysis and Design 18, 433–438.

Wilson, W.K., Yu, I.W., 1979. The use of the J integral in thermal stress crack problem. International Journal of Fracture 15, 377–387.

Yuuki, R., Cho, S.B., 1989. Efficient boundary element analysis of stress intensity factors for interface cracks in dissimilar materials. Engineering Fracture Mechanics 34, 179–188.